

Iron–Sulfur Cluster Biosynthesis: Functional Characterization of the N- and C-Terminal Domains of Human NFU[†]

Yushi Liu, Wenbin Qi, and J. A. Cowan*

Evans Laboratory of Chemistry, The Ohio State University, 100 West 18th Avenue, Columbus, Ohio 43210

Received August 29, 2008; Revised Manuscript Received October 31, 2008

ABSTRACT: Human NFU (also known as HIRIP5) has been implicated in cellular iron–sulfur cluster biosynthesis. Bacterial and yeast forms are smaller than the human protein and are homologous to the C-terminal domain of the latter. This C-terminal domain contains a pair of redox active cysteines and demonstrates thioredoxin-like activity by mediating persulfide bond cleavage of sulfur-loaded NifS (an IscS-type protein), the sulfide donor for [2Fe–2S] cluster assembly on ISU-type scaffold proteins. Herein, the affinity of full-length human NFU and the individual N- and C-terminal domains for sulfide donor and cluster scaffold proteins is assessed. The influence of the N-terminal domain on C-terminal NFU binding to NifS and persulfide reductase activity is also examined. Only the C-terminal domain is required for persulfide reductase activity, while complex formation of NifS with full-length NFU is similar to that of the C-terminal domain alone ($K_D \sim 9.7 \pm 0.7$ and $10.1 \pm 0.6 \mu\text{M}$, respectively). There is negligible affinity between the isolated C- and N-terminal domains, while the N-terminal domain has negligible affinity for either sulfide donor or cluster scaffold proteins. The temperature dependence of the binding enthalpy for formation of the complex between NifS and the C-terminal domain of NFU yields a change in molar heat capacity ($\Delta C_p \sim 138 \text{ cal mol}^{-1} \text{ K}^{-1}$) that suggests bonding at the protein–protein interface is dominated by electrostatic interactions. This is consistent with electrostatic potential maps for bacterial homologues of the N- and C-terminal domains of human NFU, which most likely reflect the structural characteristics expected for full-length human NFU.

Iron–sulfur cluster proteins are ubiquitous in all life forms (1) and have been implicated in electron transfer, gene regulation, environmental sensing, and substrate activation (1, 2). Ongoing studies have established a mechanistic framework for understanding the biosynthesis of [2Fe–2S] clusters that includes frataxin-mediated iron delivery to the Fe–S cluster scaffold protein ISU/IscU (3–7), where the term ISU is used for eukaryotic scaffold proteins and IscU for the bacterial homologues, with subsequent delivery of sulfide via the cysteinyl persulfide bond of an IscS-type protein (8, 9). The resulting cluster is then transferred to other cluster-dependent proteins (10). An alternative scaffold assembly pathway (11), involving initial transfer of sulfur with subsequent uptake of iron, is precluded by the weak binding of iron to persulfide-labeled IscU or ISU (12, 13). While iron-bound ISU has been converted to cluster-bound protein following delivery of sulfide (chemically or enzymatically) (12), reconstitution of sulfur-labeled ISU following addition of iron has not (11). To further understand the chemistry underlying reductive cleavage of the cysteinyl persulfide bond of the sulfide donor protein, a recent report characterized the persulfide reductase activity of the thioredoxin-like C-terminal domain of human NFU (14). A role for this enzyme

in iron–sulfur cluster biosynthesis is predicated on several observations. In particular, the C-terminal domain was found to bind with micromolar affinity to a sulfide donor protein with an established role in cluster biosynthesis (14), as well as promoting cleavage of the NifS persulfide bond and mediating sulfide delivery in a [2Fe–2S] cluster assembly assay using both ISU and IscU Fe–S cluster scaffold proteins. Moreover, the C-terminal domain displays a highly conserved thioredoxin-like Cys–X–X–Cys motif (Figure 1) (15–17) and is homologous to a functionally ill-defined motif at the C-terminus of *Azotobacter vinelandii* NifU (6, 15). A similar role for a CXXC motif has previously been elucidated in many other protein disulfide isomerases (PDI)¹ (18), while sequence alignment analysis shows that the C-terminal domain of NFU-type proteins is highly conserved from prokaryotes to eukaryotes, suggesting that the phylogenetically conserved NFU domain might be functionally or structurally important. An earlier report has suggested that

[†] This work was supported by a grant from the National Science Foundation (CHE-0111161 to J.A.C.).

* To whom correspondence should be addressed: Evans Laboratory of Chemistry, The Ohio State University, 100 W. 18th Ave., Columbus, OH 43210. Telephone: (614) 292-2703. Fax: (614) 292-1685. E-mail: cowan@chemistry.ohio-state.edu.

¹ Abbreviations: CD, circular dichroism; DTT, dithiothreitol; ESI-MS, electrospray ionization mass spectrometry; HEPES, *N*-(2-hydroxyethyl)piperazine-*N'*-2-ethanesulfonic acid; HIRA, histone cell cycle regulation homologue A; IPTG, isopropyl β -D-thiogalactopyranoside; *isc*, iron–sulfur cluster; ITC, isothermal titration calorimetry; LB, Luria-Bertani; MW, molecular weight; *nif*, nitrogen fixation; PAGE, polyacrylamide gel electrophoresis; PCR, polymerase chain reaction; PLP, pyridoxal 5'-phosphate; PMSF, phenylmethanesulfonyl fluoride; SDS, sodium dodecyl sulfate; TCEP, tris(2-carboxyethyl)phosphine hydrochloride; PDI, protein disulfide isomerase; Tris, tris(hydroxymethyl)aminomethane; UV, ultraviolet; LC–MS, liquid chromatography–mass spectrometry; Ni-NTA, nickel nitriloacetic acid; PDB, Protein Data Bank.

| | | |
|-------------|--|-----|
| NFU1 HUMAN | -MFIQTQDTPNPNSLKFIPGKPVLETR-TMDFPTAAAFRSPLARQLFRIEGVKSVFVFGP | 58 |
| NFU1 MOUSE | -MFIQTQDTPNPNSLKFIPGKPVLETR-TMDFPTAAAFRSPLARQLFRIEGVKSVFVFGP | 58 |
| NFU DROME | -MFIQTQDTPNPESLKFIPGVDVLGKNTYDFPNGTTAHNSPLAKLLFRVEGVKGVFFGA | 59 |
| SE NFU_N | MEIIAISETPNHNTMKVSLSEPRQDNS--STTYTAAQEGQPEFINRLFEIEGVKSIFYVL | 58 |
| SE NFU_C | ----- | |
| Ni fu SYN | ----- | |
| Ni fu AZOVI | ----- | |
| | : * : : * * : : * : . . : : * : * * * : * : | |
| NFU1 HUMAN | DFITVTKENEELDNLLKPDIIYATIMDFFASGLPLVTEETPS--GEAGSEEDDEVVAMIK | 116 |
| NFU1 MOUSE | DFITVTKENEELDNLLKPDIIYATIMDFFASGLPLVTEETPPPPGEAGSEEDDEVVAMIK | 118 |
| NFU DROME | DFVTISKQ-EGAESLIIKPEVFAVIMDFFASGLPVLNDAQPN-ADTEILEDDETVMMIK | 117 |
| SE NFU_N | DFISIDKE-DNANWNELLPQIEN---TFAKSN----- | 8 |
| SE NFU_C | -----MPTENTMTFDQV | 12 |
| Ni fu SYN | -----MELTLNNV | 8 |
| Ni fu AZOVI | -----I | 1 |
| | * * : : * : : * : : * : * * : | |
| NFU1 HUMAN | ELLDTIRIRPTVQEDGGDIVYKGFEDGIVQLKLQGSCTSCPSIIITLKNIGIQNMLQFYIPE | 176 |
| NFU1 MOUSE | ELLDTIRIRPTVQEDGGDIVYKGFEDGIVRLKLQGSCTSCPSIIITLKSIGIQNMLQFYIPE | 178 |
| NFU DROME | ELLDTIRIRPTVQEDGGDIVFMGYEGGVVVKLMQGSCTSCPSIIITLKNIGVQNMLQFYIPE | 177 |
| SE NFU_N | ----- | |
| SE NFU_C | AEVIERLRPFLLRDGGDCTLDVDEGIVKLQLHGACGTCPSSITLTKAGIERALHEEVPG | 72 |
| Ni fu SYN | ETVLDELRLPYLMADGGNVEVVELDGPVKVRLQGACGSCPSSTMTLKMGIERKLREIPE | 68 |
| Ni fu AZOVI | ETVLAAIRPTLQRDKGDVELIDVDGKNVYVVKLTGACGCMASMTLG-GIQQLIEELGE | 60 |
| | : : * * : * * : : * : : * * * : : * * * : : | |
| NFU1 HUMAN | VEGVEQVMDD-----ESDEKEANSP----- | 196 |
| NFU1 MOUSE | VEGVEQVMDD-----ESDEKEANSS----- | 199 |
| NFU DROME | VESVEQVFDEADRMIESEFERFEKNLKTLLKQEPSPGGGPH | 217 |
| SE NFU_N | ----- | |
| SE NFU_C | VIEVEQVF----- | 80 |
| Ni fu SYN | IAEVEQVL----- | 76 |
| Ni fu AZOVI | FVKVIPVSAAA-----HAQMEV----- | 77 |
| | . * * | |

FIGURE 1: Multiple-sequence alignment of selected NFU proteins from *Homo sapiens* (Hs), *Mus musculus* (Mm), *Drosophila melanogaster* (Dm), *Synechocystis* PCC6803 (Syn), *Azotobacter vinelandii* (Av), and *Staphylococcus epidermidis* (Se). N-Terminal similarity (human protein numbering of 1–114) was compared across Hs NFU1, Mm NFU1, Dm NFU, and the putative Se NFU-N protein. C-Terminal similarity (human protein numbering of 115–196) was compared across Hs NFU1, Mm NFU1, Syn NifU, Av NifU, and the putative Se NFU-C protein. Identical, conserved, and semiconserved residues are marked with asterisks, colons, and periods, respectively. Conserved Cys residues are highlighted in yellow. The alignment was produced by ClustalW (42) and was manually modified.

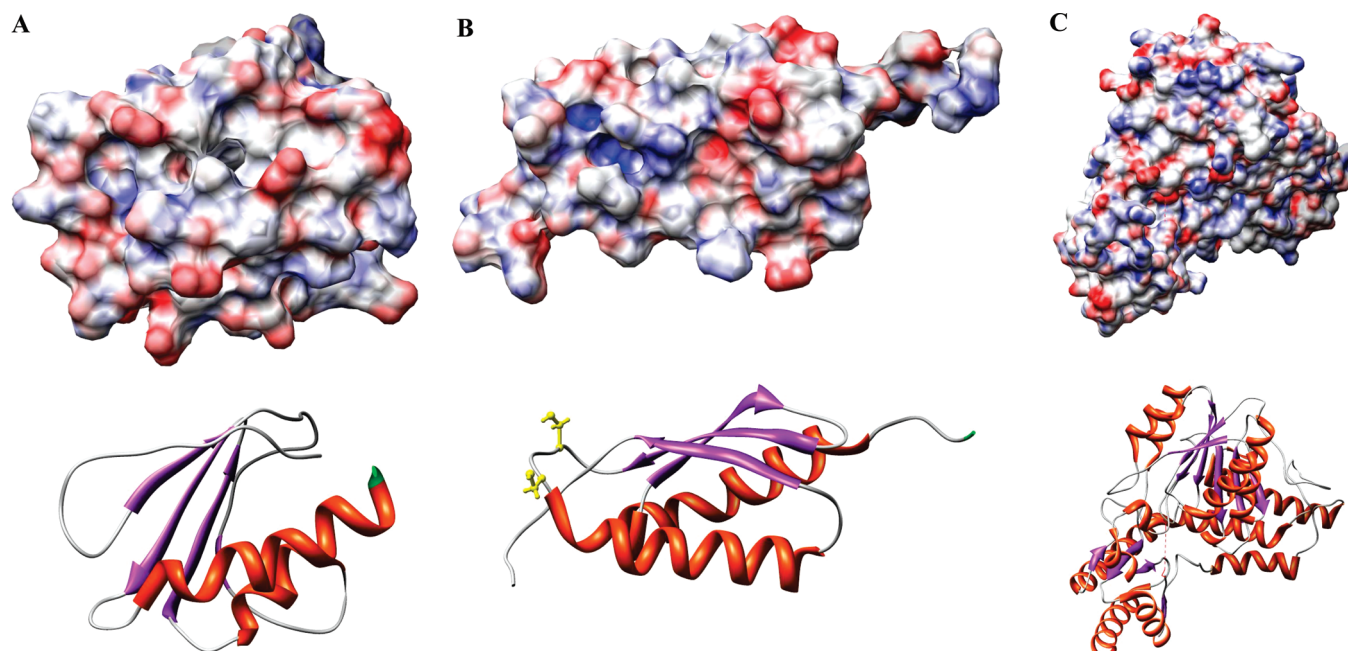


FIGURE 2: Structural representation and electrostatic potential maps of the N- and C-terminal sequence homologues of Se and Tm NifS. (A) Structure of Se NFU-N (PDB entry 2K1H). The last few residues are colored green. (B) Structure of Se NFU-C (PDB entry 1XHJ). Cysteines are shown in yellow ball-and-stick representations, while the first few residues are colored green. The green domains in panels A and B would be connected in a model of full-length human NFU. (C) Structure of Tm NifS (PDB entry 1EG5). The dashed line connects Thr320 and His333 and indicates the position of residues 321–332 that are missing as a result of the conformational flexibility of this loop domain, including the sulfide donor Cys324. Electrostatic surface potential maps were calculated with APBS (43), while the structural representations and electrostatic potential surfaces were visualized with Chimera (44).

human NFU serves as an alternative scaffold protein in iron–sulfur cluster assembly (20) and is discussed in the context of the findings reported here.

NFU has highly conserved homologues in both prokaryotes and eukaryotes (19–22), suggesting a significant cellular role for this protein. Gene knockout experiments in yeast

demonstrate NFU to be essential for iron–sulfur cluster biosynthesis (3), while complementary studies have begun to probe the functional chemistry of this protein in a variety of organisms (20–22). Human NFU has been implicated in several physiological pathways and may be multifunctional (20, 22, 23), consistent with identification of two distinct isoforms of human NFU (20). One isoform is localized in the mitochondrion, and the other, lacking the N-terminal domain, is localized in the cytosol and nucleus (20). Interaction with HIRA (histone cell cycle regulation homologue A) has been observed and has been suggested to play a role in transcriptional regulation at the level of local chromatin structure (22, 24). Recent studies also show that human NFU could interact with laforin, mutations of which lead to lafora disease (25), while genetic evidence had earlier suggested a role for NFU in iron homeostasis, perhaps in iron–sulfur cluster assembly (3).

In this paper, the catalytic and partner binding properties of the full-length NFU protein are compared to those of the N- and C-terminal domains, and the influence of the N-terminal domain on C-terminal cysteinyl persulfide reductase activity is assessed in the context of [2Fe-2S] cluster assembly in ISU-type proteins. Structural comparison is made with bacterial homologues of the N- and C-terminal domains of human NFU (Figure 2), which also provide insight into structural features that are most likely associated with the full-length human protein, as well as other bacterial and plant homologues (19–21). A possible binding interface is proposed for formation of a complex with the sulfur donor protein that is supported by comparisons of electrostatic potential maps of protein surfaces and the calorimetrically determined heat capacity for binding.

MATERIALS AND METHODS

General Chemicals. All restriction enzymes were obtained from Invitrogen (Carlsbad, CA). The Qiaquick gel extraction kit and Ni-NTA columns were from Qiagen (Valencia, CA), and BL21(DE3) cells and pET28 vectors were from Novagen (Madison, WI). Primers were obtained from Integrated DNA Technologies Inc. (Coralville, IA), and CM 32 and DE 52 ion exchange resins were from Whatman (Aston, PA). Homogeneous-20 precast polyacrylamide gels and G-25 resin were obtained from Pharmacia (Peapack, NJ).

Cloning, Expression, and Purification of Proteins. Experimental details are provided in the Supporting Information.

Circular Dichroism of Full-Length NFU and the N- and C-Terminal Domains. The secondary structure was evaluated both experimentally by circular dichroism methods and by prediction based on sequence analysis. Spectra were collected with an Aviv model 202 circular dichroism spectrometer at 25 °C at a resolution of 1 nm in a cuvette with a path length of 10 mm. The wavelength range was from 200 to 350 nm for each spectrum that was recorded, and data were obtained five times and averaged. Spectra for protein samples (0.85 μ M full-length NFU, 1.2 μ M N-terminal domain, and 1.53 μ M C-terminal domain) that had been dialyzed into 20 mM sodium phosphate buffer (pH 7.5) were recorded. The averaged baseline-corrected spectra were deconvoluted by use of the online software K2D (<http://www.embl-heidelberg.de/~andrade/k2d/>), and the secondary structure of the N-terminal domain of NFU was predicted from its sequence

using the Protein Structure Prediction Server (PSIPRED, <http://bioinf.cs.ucl.ac.uk/psipred/psiform.html>). The predicted secondary structure and the deconvoluted secondary structure were compared.

NFU-Promoted IscU Reconstitution. Both NFU and IscU were dialyzed against 50 mM Tris-HCl (pH 7.5) and then incubated with excess DTT, which was subsequently removed by ultrafiltration (Amicon) under strict anaerobic conditions. NFU (400 μ M) and IscU (200 μ M) were then incubated with 0.8 mM Fe²⁺, 2 mM L-cysteine, and 7 μ M NifS. After 2 h, the mixture was loaded onto a Sephadex G-25 gel filtration column equilibrated with argon-purged 50 mM Tris-HCl (pH 7.5). For His-tagged IscU, the colored fractions of holo IscU were concentrated. If non-His-tagged IscU was used, the protein fractions were loaded onto a Ni-NTA column and washed with 3 volumes of argon-purged 50 mM Tris-HCl (pH 7.5) buffer. The washed and eluted fractions were combined and loaded onto an anion exchange column (DE 52). A 50 mM Tris-HCl/300 mM NaCl (pH 7.5) buffer was used to elute the reconstituted non-His-tagged IscU. The colored fractions containing holo IscU (as judged by SDS–PAGE) were pooled and concentrated.

UV–visible spectra were recorded with a cuvette with a path length of 1.0 cm on a Hewlett-Packard 8452A diode array spectrophotometer using the Online Instrument Systems (OLIS) 4300S operating system software.

Kinetic Analysis of IscU Reconstitution Promoted by both Human NFU and the C-Terminal Domain of NFU. The fully reduced forms of NFU and IscU were prepared as described above. Subsequently, the following components were mixed anaerobically, where final concentrations are indicated: 50 μ M IscU and 100 μ M NFU (or 50 μ M C-terminal NFU) with 200 μ M ferrous iron and 500 μ M L-cysteine. Finally, *Thermotoga maritima* NifS was injected into the mixture to a concentration of 3.6 μ M. A Hewlett-Packard 8452A diode array spectrophotometer was used to monitor the time dependence of iron–sulfur cluster assembly on IscU, and control experiments in the absence of NFU, IscU, and NifS were also conducted.

The absorbance at 412 nm was monitored over a period of 120 min, and kinetic data were fit to a first-order decay profile and compared with the NFU reconstitution data for IscU. Human ISU was studied in a similar fashion. A solution of 90 μ M reduced human ISU and 180 μ M reduced human NFU (or C-terminal human NFU) was mixed anaerobically. Subsequently, 200 μ M Fe²⁺, 500 μ M L-cysteine, and 3.6 μ M *T. maritima* NifS were mixed, and a Hewlett-Packard 8452A diode array spectrophotometer was used to monitor the time dependence for the reaction leading to iron–sulfur cluster assembly on IscU. Control experiments in the absence of NFU, IscU, and NifS were also conducted.

Quantitation of Human NFU Binding to NifS via Isothermal Titration Calorimetry. ITC measurements were carried out at 25 °C on a MicroCal VP-ITC system. The titrant and sample solution were dialyzed against the same buffer solution [20 mM HEPES (pH 7.5)], and both solutions were thoroughly degassed under vacuum and supplemented with 1 mM TCEP. A 10 μ L volume of the titrant (750 μ M human NFU) was injected into the sample cell (50 μ M NifS) over a period of 20 s. The contents of the sample cell were stirred at 300 rpm to ensure rapid and complete reaction, with a 300 s interval between subsequent injections. Up to 3.5 equiv

of titrant was added to ensure no further formation of the NFU–NifS complex. A control reaction in which the titrant was injected into the cell containing only the buffer solution was performed and subtracted as the background. The data were analyzed and fit to a one-site binding model.

A similar experiment was performed when the N- and C-terminal truncated domains of NFU were used. The data were also fit to a one-site binding model except in this case 25 μ M NifS and 1.1 mM C-terminal NFU were used. Variable-temperature experiments were also carried out at 10, 35, and 45 °C to determine the change in the molar heat capacity (ΔC_p).

RESULTS AND DISCUSSION

Cloning, Expression, and Purification of Full-Length Human NFU and the N- and C-Terminal Domains. Full-length NFU and the N-terminal (residues 1–132) and C-terminal (residues 133–215) domains (Figure 1), lacking mitochondrial targeting sequences, were amplified by PCR methods and cloned into a pET-28b(+) plasmid for protein expression. An N-terminal His₆ tag facilitated purification, and purity was confirmed by SDS–PAGE analysis. All protein samples proved to be satisfactory by mass spectral analysis, after accounting for loss of the N-terminal methionine. Mass spectroscopic analysis of full-length human NFU showed one major peak at 23831 Da, matching the molecular mass of His-tagged human NFU without the amino-terminal Met, while the ESI-MS spectrum for the C-terminal domain showed a major peak at 11265 Da (also lacking an N-terminal Met). A mass difference of 2 Da between observed and expected masses for the full-length and C-terminal NFU proteins most likely reflects formation of an intramolecular disulfide bond between the contiguous cysteines found in the CXXC motif of both full-length and C-terminal human NFU. Similarly, the expected mass was obtained for the purified recombinant N-terminal domain.

An oxygen sensitivity assay was used to determine the best storage conditions for reduced NFU. After reduction with DTT (subsequently removed by ultrafiltration), human NFU was reacted with DTNB to determine the number of equivalents of free thiol. The molar ratio of free thiol to protein was initially determined to be \sim 2. When the mixture was left open to the air at ambient temperature, the ratio of free thiol to protein decreased to 0.1, indicating cysteinyl oxidation. Reduced human NFU may be stored for \sim 8 h without oxidation if stored anaerobically at 4 °C.

Circular Dichroism of NFU and Its N- and C-Terminal Domains. CD spectra (Supporting Information) were fit by use of the online fitting software K2D to determine the percentage of secondary structural components, and the data are summarized in Table 1. Resolving the CD spectra provided a secondary structure composition of 31% α -helix, 12% β -sheet, and 57% random coil for full-length NFU, 30% α -helix, 17% β -sheet, and 53% random coil for the C-terminal domain, and 30% α -helix, 14% β -sheet, and 56% random coil for the N-terminal domain. These results were found to be consistent with predictions based on the use of the PSIPRED program, which predicted a composition of 33% α -helix, 18% β -sheet, and 50% random coil for full-length NFU, 32% α -helix, 18% β -sheet, and 50% random coil for the C-terminal domain, and 31% α -helix, 12%

Table 1: Secondary Structure Content of Full-Length Human NFU, the N- and C-Terminal Domains of Human NFU, and Bacterial Homologues^a

| | A | B | C | D | E |
|-----------------|-----|-----|-----|-----|-----|
| α -helix | 31% | 30% | 30% | 23% | 40% |
| β -sheet | 12% | 14% | 17% | 21% | 21% |
| random coil | 57% | 56% | 53% | 56% | 39% |

^a Experimental secondary structures of (A) full-length human NFU, (B) the N-terminal domain of human NFU, (C) the C-terminal domain of human NFU, (D) the N-terminal homologue from *S. epidermidis* (PDB entry 2K1H), and (E) the C-terminal homologue from *S. epidermidis* (PDB entry 1XJH). For A–C, the CD spectra were deconvoluted using K2D. Secondary structures for D and E were obtained from reported NMR structural data (PDB entries 2K1H and 1XJH, respectively).

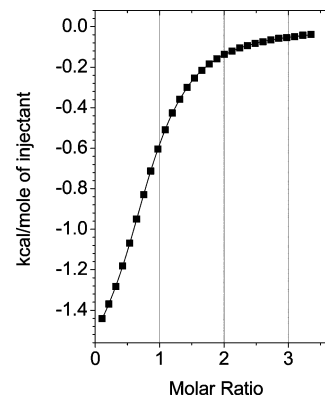


FIGURE 3: ITC profile for NifS binding to full-length human NFU at 25 °C. Samples were prepared in degassed 20 mM HEPES buffer (pH 7.5). Fitting yielded the following: stoichiometry $n \sim 0.92$, $\Delta H \sim -1.7$ kcal/mol, $\Delta S \sim 15.3$ cal K^{−1} mol^{−1}, and $K_D \sim 9.7$ μ M.

β -sheet, and 57% random coil for the N-terminal domain. For comparison, the secondary structures of *S. epidermidis* homologues of the N- and C-terminal domains of human NFU (Figure 2) are also summarized in Table 1.

Quantitation of Human NFU Binding to NifS by Isothermal Titration Calorimetry. Previously, we have reported formation of a complex between the C-terminal domain of NFU and NifS, with a K_D of \sim 10.1 μ M (14). Binding was observed to be both entropically and enthalpically favorable and was similar for His₆- and non-His-tagged protein. No direct interaction was detected between the C-terminal domain of NFU and either *Hs* ISU or *Tm* IscU. The use of the *Tm* NifS homologue as a substitute for human NFS, which is not readily available (26), is justified by the sequence and structural similarity of this family of proteins (the structures are often superimposable) (9, 27, 28), and the functionally relevant chemistry of *Tm* NifS with both human ISU and NFU. Moreover, *Tm* NifS shows similar binding affinities for both *Tm* IscU and human ISU proteins (manuscript submitted for publication), with no evidence of differentiation between species. IscS-type proteins are found throughout the cell and are conserved among species, suggesting flexibility in accommodating various substrates in their interaction surfaces.

The interaction between full-length NFU and NifS was quantified by isothermal titration calorimetry, yielding a K_D of \sim 9.7 μ M for a 1:1 complex of human NFU with NifS (Figure 3). Entropy and enthalpy contributions are summarized in Table 2 and demonstrate again that binding is both entropically and enthalpically favorable. The similarity

Table 2: Summary of Thermodynamic Parameters for Binding of Human NFU and Its C-Terminal Domain to *Tm* NifS^a

| | no. of binding sites | K_D (μ M) | ΔH (kcal/mol) | ΔS (eu) | ref |
|---------------------------------|----------------------|------------------|-----------------------|-----------------|-----------|
| full-length NFU– <i>Tm</i> NifS | 0.92 ± 0.02 | 9.7 ± 0.7 | -1.69 ± 0.5 | 15.3 | this work |
| C-terminal NFU– <i>Tm</i> NifS | 0.95 ± 0.05 | 10.1 ± 1.4 | -1.8 ± 0.3 | 16.7 | 14 |

^a No binding of N-terminal human NFU to *Tm* NifS was observed, and the N-terminal domain had no significant influence on binding of either the full-length or C-terminal NFU proteins to NifS.

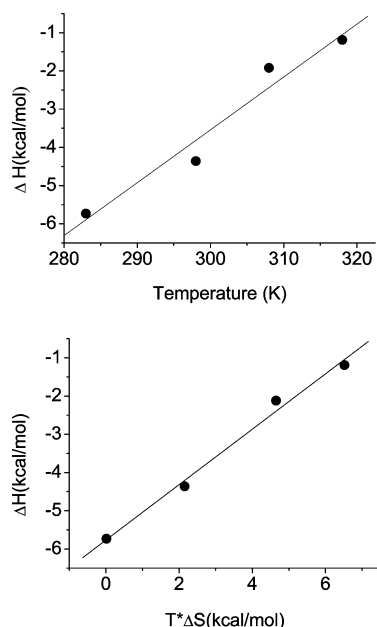


FIGURE 4: Results from temperature-dependent ITC experiments showing the dependence of ΔH on temperature (top). The data were fit by linear regression analysis to the equation $\Delta H_M = \Delta C_p T + \Delta H_0$ (34) to yield a change in molar heat capacity, ΔC_p , of ~ 138 cal mol⁻¹ K⁻¹. A plot of ΔH_M vs $T\Delta S_M$ (bottom) yielded a ΔG of approximately -5.8 kcal/mol and demonstrates the insensitivity of free energy to temperature that in turn is indicative of compensatory enthalpic and entropic changes.

in K_D values for full-length and C-terminal protein suggests that the NifS binding site is located within the C-terminal domain of NFU. However, no direct interaction was detected between NFU and either *Hs* ISU or *Tm* IscU.

Temperature Dependence of NifS and C-Terminal NFU Binding. Having established formation of a complex between NifS and NFU, we further investigated the structural factors that promote binding of NifS and NFU by means of temperature-dependent calorimetry experiments to determine the polarity of the binding interface. The change in molar heat capacity often reflects the reorganization of solvent molecules due to the protein partner binding. A negative change in molar heat capacity following formation of a protein complex is usually attributed to hydrophobic interactions (29–31), while a positive change in molar heat capacity following protein–protein interactions is rare (32–34). C-Terminal NFU was used as a model to investigate this topic, since it was more readily obtained in higher yield, relative to full-length NFU, while other data reported herein suggest the binding interface involves the C-terminal domain exclusively. ITC experiments were performed with the same preset parameters, the only difference being the background temperature. In this case, only the binding enthalpy and entropy were affected by temperature, while the binding affinity remained almost the same (Figure 4).

Two plots were constructed to evaluate the factors underlying complex formation. The first graph was con-

structed with temperature (in kelvin) as the x -axis and binding enthalpy as the y -axis. The graph indicated that the change in binding enthalpy was dependent on temperature, so data were fit by linear regression analysis to the equation $\Delta H_M = \Delta C_p T + \Delta H_0$ (34), yielding a change in molar heat capacity, ΔC_p , of ~ 138 cal mol⁻¹ K⁻¹ (Figure 4). Positive changes in molar heat capacity are usually attributed to a reduction in the number of surface-exposed polar groups as a result of formation of a salt bridge between charged residues (34, 35). Another factor that most likely contributes to the positive entropy change is the loss of solvent molecules on the binding surface that accompanies complex formation. A plot of ΔH_M versus $T\Delta S_M$ resulted in a straight line (Figure 4), and fitting to the equation $\Delta H_M = T\Delta S_M + \Delta G$ yielded a ΔG of approximately -5.77 kcal/mol, which was not sensitive to the variation of the temperature. Apparently, there are compensatory enthalpic and entropic changes involved in the binding process.

Binding of the N-Terminal Domain of NFU to the C-Terminal Domain of NFU and/or NifS. An ITC study of the direct binding of the individual N- and C-terminal domains suggested the absence of significant interactions between them. The possibility that a binding event did not produce a heat change could not be ruled out, so additional experiments were performed. Specifically, the competitive binding of N-terminal NFU to a complex of NifS and C-terminal NFU was studied by ITC. The similarity in K_D values for full-length NFU and the C-terminal domain toward NifS suggested that the N-terminal domain did not bind to NifS, a conclusion that was supported by these competitive binding ITC experiments. Accordingly, if the N-terminal domain were to bind to the C-terminal domain and cause it to be released from NifS, then this should result in an enthalpy change; however, no such change was observed.

Kinetics of ISU/IscU Cluster Reconstitution Mediated by Full-Length NFU, and the N- and C-Terminal Domains. In prior studies, we have demonstrated the C-terminal domain of NFU to mediate the release of inorganic sulfide from persulfide-labeled *Tm* NifS (a sequence and structural homologue, and representative of the IscS family) (9, 27, 28). Formation of a complex between full-length NFU and NifS was demonstrated by isothermal titration calorimetry, with a measured K_D of ~ 9.7 μ M (Figure 3). Previously, NifS was shown to mediate reconstitution of the ISU-bound iron–sulfur cluster by serving as the sulfur donor (4, 14, 36). The ability of NFU to promote reductive cleavage of the NifS persulfide bond, and physiologically relevant binding to NifS, suggests a role for NFU in cluster biogenesis as a reductase that promotes formation and delivery of inorganic sulfide to the ISU scaffold protein through direct interaction with NifS. Direct involvement in cluster biosynthesis is supported by the reconstitution data shown in Figure 5. To better characterize the roles of the N- and C-terminal domains, relative to full-length NFU, the kinetics of [2Fe-2S] cluster formation

Table 3: Observed Rate Constants for NFU-Mediated Assembly of Human ISU and *Tm* IscU

| | k_{obs} (min ⁻¹) | cluster yield (%) | ref |
|--------------------------------------|---------------------------------------|-------------------|-----------|
| C-terminal NFU- <i>Hs</i> D37A ISU | 0.015 ± 0.005 | 79 | 14 |
| C-terminal NFU- <i>Tm</i> D40A IscU | 0.017 ± 0.003 | 69 | 14 |
| full-length NFU- <i>Hs</i> D37A ISU | 0.016 ± 0.004 | 82 | this work |
| full-length NFU- <i>Tm</i> D40A IscU | 0.019 ± 0.006 | 71 | this work |

on two representative ISU-type proteins (from *T. maritima* and humans) has been characterized.

Time-dependent kinetic studies of iron-sulfur cluster assembly revealed no cluster formation under the conditions used in the absence of NifS, IscU, or NFU. A slight increase in absorbance was observed in the absence of IscU as a result of the formation of ferrous sulfide. These experiments demonstrated the essential role of NFU in iron-sulfur cluster biosynthesis, and kinetic parameters are summarized in Table 3. Both full-length human NFU and the C-terminal domain yielded similar results, suggesting that the C-terminal domain was necessary and sufficient to fulfill the cleavage function. Reconstitution yields of *T. maritima* IscU were ~69 and ~71%, respectively, when mediated by either the C-terminal domain or full-length NFU, based on the published extinction coefficient (37, 38).

To determine if similar reactivity arose with the human protein, the human homologue (ISU) was studied. Both full-length NFU and the C-terminal domain were used to reconstitute human ISU. The reaction profile was similar to that observed for the reconstitution of *Tm* IscU, and the data were readily fit to a first-order profile. Again, both the C-terminal domain and the full-length human NFU were used, and each was found to be essential for iron-sulfur cluster assembly on human ISU, with reconstitution yields of ~79 and ~82%, respectively. Results from the kinetic experiments are summarized in Table 3, and the overall similarity in rate constants for human and *Tm* ISU-type proteins (Table 1) supports the structural homology of the ISU proteins and their partner recognition sites.

The N-terminal domain of NFU proved ineffective in promoting reconstitution of either *Tm* IscU or human ISU. Moreover, the N-terminal domain had no effect on the reconstitution process promoted by the C-terminal domain of NFU.

Functional Chemistry of the C-Terminal Domain. While a prior report has described reconstitution of human NFU from cell extracts, the reported yield of the [4Fe-4S] holo form was low, the Mossbauer spectrum unusual, and further cluster transfer activity undocumented (20). Our attempts to reproduce this were unsuccessful, using either full-length or C-terminal protein with a variety of reconstitution conditions. Our efforts to quantitate binding of ferric and ferrous ion to human NFU by isothermal titration calorimetry (ITC) and fluorescence measurements revealed weak binding (millimolar K_D) at best (14). If NFU can in fact be reconstituted with the cluster under appropriate conditions, then this would speak to a dual functional role with very distinct activities for each form.

While human NFU may serve several cellular roles, the data reported herein show that NFU binds to NifS and reduces the persulfide bond on activated NifS (following formation of the persulfide bond by abstraction of S from

the Cys amino acid), yielding inorganic sulfide on a time frame that is compatible with Fe-S cluster assembly. Such results are consistent with a general mechanism that has been proposed for the iron-sulfur cluster biosynthesis process on human ISU: (1) frataxin-mediated delivery of iron to ISU and formation of a nucleation site for [2Fe-2S] cluster formation (12, 13) and (2) delivery of inorganic sulfide by a NifS-like donor protein (12), where reductive cleavage of the persulfide bond is mediated by NFU. Highly conserved homologues to human NFU are found in a multitude of organisms. Consequently, the functional roles for NFU are most likely important and conserved, one of which appears to be the involvement of the C-terminal domain in iron-sulfur cluster biogenesis, while the N-terminal domain apparently serves a distinct function.

Structural and Sequence Considerations. Figure 1 demonstrates that the eukaryotic NFU family of proteins shows significant sequence homology across a variety of organisms. The N- and C-terminal domains appear to serve distinct roles, with the C-terminus implicated in iron-sulfur cluster assembly and shown to both bind to the sulfide donor protein and mediate sulfide delivery through its persulfide reductase activity. Bacterial homologues of the N- and C-terminal domains have been identified, though often with unassigned functions. Structural information is available on two proteins from *S. epidermidis* (herein represented as Se NFU-N and NFU-C, respectively) that are highly homologous in sequence to the N- and C-terminal domains of human NFU (Figure 1), so the structures of these two proteins most likely demonstrate key structural features of the C-terminal, N-terminal, and full-length human NFU proteins. As shown in Figure 2A, the two cysteines in the CXXC motif are located between an α -helix (α_2) and a β -sheet (β_2), and both are solvent-exposed. The electrostatic potential map of *Se* NFU-C (Figure 2A) shows several charged patches neighboring the two exposed Cys residues. The electrostatic map for *Tm* NifS (Figure 2C) shows possible complementary charged domains around Cys 324 that is active in persulfide bond formation, allowing for NFU to bind to the sulfur donor site via salt bridge formation in a manner that is consistent with heat capacity measurements.

The apparently distinct functions of the N- and C-terminal domains are reflected by the variety of processes in which NFU has been implicated in human physiology. Prior studies have implicated NFU with the DiGeorge and velocardifacial syndromes (24, 39, 40), as well as progressive myoclonus epilepsy, or Lafora-type disease (41). This conserved protein is ubiquitously present in a variety of organisms (3), suggesting an important role in the life cycle of cells. In fact, many organisms contain more than one form of NFU. Research on *Arabidopsis thaliana* has demonstrated the existence of five different isoforms of NFU (19), NFU 1–5. *At* NFU 1–3 proteins can be classified as a new type of NFU, since each of them has two repeated NFU domains, one of which has lost the conserved CXXC motif. This class of NFU is believed to be unique to plants and is localized in the plastids. In contrast, *At* NFU 4 and 5 fall into the class of mitochondrial-type NFUs, and indeed, *At* NFU 4 has been shown to target mitochondria (19).

Clearly, this is an important protein family that exhibits varied and novel functional roles. Developing a more detailed

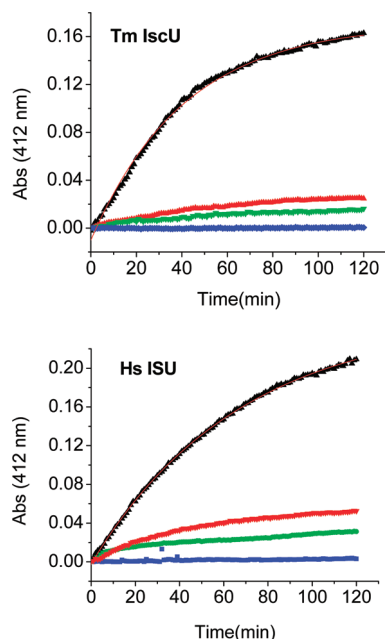


FIGURE 5: Time dependence of iron-sulfur cluster reconstitution in *Tm* D40A IscU and human D37A ISU using full-length human NFU as the persulfide reductase (black). Control reactions are shown for experiments carried out in the absence of full-length NFU (red), in the absence of IscU (green), and in the absence of NifS (blue).

molecular understanding of its chemistry in the context of cellular iron chemistry is an ongoing research goal.

SUPPORTING INFORMATION AVAILABLE

Experimental details for the cloning, expression, and purification of full-length human NFU and the N- and C-terminal domains, purification of other proteins described, mass spectrometry experiments, and CD spectra for full-length human NFU and the N- and C-terminal domains. This material is available free of charge via the Internet at <http://pubs.acs.org>.

REFERENCES

- Beinert, H., Holm, R. H., and Munck, E. (1997) Iron-sulfur clusters: Nature's modular, multipurpose structures. *Science* 277, 653–659.
- Beinert, H. (2000) Iron-sulfur proteins: Ancient structures, still full of surprises. *J. Biol. Inorg. Chem.* 5, 2–15.
- Schilke, B., Voisine, C., Beinert, H., and Craig, E. (1999) Evidence for a conserved system for iron metabolism in the mitochondria of *Saccharomyces cerevisiae*. *Proc. Natl. Acad. Sci. U.S.A.* 96, 10206–10211.
- Urbina, H. D., Silberg, J. J., Hoff, K. G., and Vickery, L. E. (2001) Transfer of Sulfur from IscS to IscU during Fe/S Cluster Assembly. *J. Biol. Chem.* 276, 44521–44526.
- Kato, S.-I., Mihara, H., Kurihara, T., Takahashi, Y., Tokumoto, U., Yoshimura, T., and Esaki, N. (2002) Cys-328 of IscS and Cys-63 of IscU are the sites of disulfide bridge formation in a covalent bound IscS/IscU complex: Implications for the mechanism of iron-sulfur cluster assembly. *Proc. Natl. Acad. Sci. U.S.A.* 99, 5948–5952.
- Frazzon, J., and Dean, D. R. (2003) Formation of iron-sulfur clusters in bacteria: An emerging field in bioinorganic chemistry. *Curr. Opin. Chem. Biol.* 7, 166–173.
- Garland, S. A., Hoff, K., Vickery, L. E., and Culotta, V. C. (1999) *Saccharomyces cerevisiae* ISU1 and ISU2: Members of a Well-conserved Gene Family for Iron-Sulfur Cluster Assembly. *J. Mol. Biol.* 294, 897–907.
- Zheng, L., White, R. H., Cash, V. L., and Dean, D. R. (1994) Mechanism for the desulfurization of L-cysteine catalyzed by the nifS gene product. *Biochemistry* 33, 4714–4720.
- Kaiser, J. T., Clausen, T., Bourenkow, G. P., Bartunik, H. D., Steinbacher, S., and Huber, R. (2000) Crystal structure of a NifS-like protein from *Thermotoga maritima*: Implications for iron sulphur cluster assembly. *J. Mol. Biol.* 297, 451–464.
- Wu, S. P., Wu, G., Surerus, K. K., and Cowan, J. A. (2002) Iron-sulfur cluster biosynthesis. Kinetic analysis of [2Fe-2S] cluster transfer from holo ISU to apo Fd: Role of redox chemistry and a conserved aspartate. *Biochemistry* 41, 8876–8885.
- Smith, A. D., Agar, J. N., Johnson, K. A., Frazzon, J., Amster, I. J., Dean, D. R., and Johnson, M. K. (2001) Sulfur transfer from IscS to IscU: The first step in iron-sulfur cluster biosynthesis. *J. Am. Chem. Soc.* 123, 11103–11104.
- Nuth, M., Yoon, T., and Cowan, J. A. (2002) Iron-sulfur cluster biosynthesis: Characterization of iron nucleation sites for assembly of the [2Fe-2S]²⁺ cluster core in IscU proteins. *J. Am. Chem. Soc.* 124, 8774–8775.
- Yoon, T., and Cowan, J. A. (2003) Iron-sulfur cluster biosynthesis. Characterization of frataxin as an iron donor for assembly of [2Fe-2S] clusters in ISU-type proteins. *J. Am. Chem. Soc.* 125, 6078–6084.
- Liu, Y., and Cowan, J. A. (2007) Iron Sulfur Cluster Biosynthesis. Human NFU Mediates Sulfide Delivery to ISU in the Final Step of [2Fe-2S] Cluster Assembly. *Chem. Commun.*, 3192–3194.
- Frazzon, J., Fick, J. R., and Dean, D. R. (2002) Biosynthesis of iron-sulfur clusters is a complex and highly conserved process. *Biochem. Soc. Trans.* 30, 680–685.
- Holmgren, A. (1989) Thioredoxin and Glutaredoxin Systems. *J. Biol. Chem.* 264, 13963–13966.
- Yano, H., Kuroda, S., and Buchanan, R. B. (2002) Disulfide proteome in the analysis of protein function and structure. *Proteomics* 2, 1090–1096.
- Ellgaard, L., and Ruddock, L. W. (2005) The human protein disulfide isomerase family: Substrate interactions and functional properties. *EMBO Rep.* 6, 28–32.
- Leon, S., Touraine, B., Ribot, C., Briat, J. F., and Lobreaux, S. (2003) Iron-sulphur cluster assembly in plants: Distinct NFU proteins in mitochondria and plastids from *Arabidopsis thaliana*. *Biochem. J.* 371, 823–830.
- Tong, W. H., Jameson, G. N., Huynh, B. H., and Rouault, T. A. (2003) Subcellular compartmentalization of human Nfu, an iron-sulfur cluster scaffold protein, and its ability to assemble a [4Fe-4S] cluster. *Proc. Natl. Acad. Sci. U.S.A.* 100, 9762–9767.
- Nishio, K., and Nakai, M. (2000) Transfer of iron-sulfur cluster from NifU to apoferritin. *J. Biol. Chem.* 275, 22615–22618.
- Lorain, S., Lecluse, Y., Scamps, C., Mattei, M. G., and Lipinski, M. (2001) Identification of human and mouse HIRA-interacting protein-5 (HIRIP5), two mammalian representatives in a family of phylogenetically conserved proteins with a role in the biogenesis of Fe/S proteins. *Biochim. Biophys. Acta* 1517, 376–383.
- Ganesh, S., Tsurutani, N., Suzuki, T., Ueda, K., Agarwala, K. L., Osada, H., Delgado-Escueta, A. V., and Yamakawa, K. (2003) The Lafora disease gene product laforin interacts with HIRIP5, a phylogenetically conserved protein containing a NifU-like domain. *Hum. Mol. Genet.* 12, 2359–2368.
- Magnaghi, P., Roberts, C., Lorain, S., Lipinski, M., and Scambler, P. J. (1998) HIRA, a mammalian homologue of *Saccharomyces cerevisiae* transcriptional co-repressors, interacts with Pax3. *Nat. Genet.* 20, 74–77.
- Subramaniam Ganesh, N. T., Suzuki, T., Ueda, K., Lal Agarwala, K., Osada, H., Delgado-Escueta, A. V., and Yamakawa, K. (2003) The Lafora disease gene product laforin interacts with HIRIP5, a phylogenetically conserved protein containing a NifU-like domain. *Hum. Mol. Genet.* 12, 2359–2368.
- Li, K., Tong, W.-H., Hughes, R. M., and Rouault, T. A. (2006) Roles of the Mammalian Cytosolic Cysteine Desulfurase, ISCS, and Scaffold Protein, ISCU, in Iron-Sulfur Cluster Assembly. *J. Biol. Chem.* 281, 12344–12351.
- Cupp-Vickery, J. R., Urbina, H., and Vickery, L. E. (2003) Crystal structure of IscS, a cysteine desulfurase from *Escherichia coli*. *J. Mol. Biol.* 330, 1049–1059.
- Percudani, R., and Peracchi, A. (2003) A genomic overview of pyridoxal-phosphate-dependent enzymes. *EMBO Rep.* 4, 850–854.
- Lin, Z., Schwartz, F. P., and Eisenstein, E. (1995) The hydrophobic nature of GroEL-substrate binding. *J. Biol. Chem.* 270, 10111–10114.
- Murphy, K. P., Privalov, P. L., and Gill, S. J. (1990) Common Feature of Protein Unfolding and Dissolution of Hydrophobic Compounds. *Science* 247, 559–561.

31. Manunya, N. (2004) Mechanism of Fe-S Cluster Biosynthesis: The [2Fe-2S] IscU as a Model Scaffold. Ph.D. Thesis, pp 22–26, The Ohio State University, Columbus, OH.
32. Niedzwiecka, A., Stepinski, J., Darzynkiewicz, E., Sonenberg, N., and Stolarski, R. (2002) Positive heat capacity change upon specific binding of translation initiation factor eIF4E to mRNA 5' cap. *Biochemistry* 41, 12140–12148.
33. Hileman, R. E., Jennings, R. N., and Linhardt, R. J. (1998) Thermodynamic analysis of the heparin interaction with a basic cyclic peptide using isothermal titration calorimetry. *Biochemistry* 37, 15231–15237.
34. Zhou, Y.-L., Liao, J.-M., Du, F., and Liang, Y. (2005) Thermodynamics of the interaction of xanthine oxidase with superoxide dismutase studied by isothermal titration calorimetry and fluorescence spectroscopy. *Thermochim. Acta* 426, 173–178.
35. Janin, J. (1997) The kinetics of protein-protein recognition. *Proteins* 28, 153–161.
36. Balk, J., and Lill, R. (2004) The cell's cookbook for iron–sulfur clusters: Recipes for fool's gold? *ChemBioChem* 5, 1044–1049.
37. Mansy, S. S., Wu, G., Surerus, K. K., and Cowan, J. A. (2002) Iron-sulfur cluster biosynthesis. *Thermatoga maritima* IscU is a structured iron-sulfur cluster assembly protein. *J. Biol. Chem.* 277, 21397–21404.
38. Foster, M. W., Whang, J., Penner-Hahn, J. E., Surerus, K. K., and Cowan, J. A. (2000) A mutant Human IscU Protein Contains a Stable [2Fe-2S] Center of Possible Functional Significance. *J. Am. Chem. Soc.* 122, 6805–6806.
39. Lorain, S., Quivy, J. P., Monier-Gavelle, F., Scamps, C., Lecluse, Y., Almouzni, G., and Lipinski, M. (1998) Core histones and HIRIP3, a novel histone-binding protein, directly interact with WD repeat protein HIRA. *Mol. Cell. Biol.* 18, 5546–5556.
40. Scambler, P. J. (2000) The 22q11 deletion syndromes. *Hum. Mol. Genet.* 9, 2421–2426.
41. Berkovic, S. F., Andermann, F., Carpenter, S., and Wolfe, L. S. (1986) Progressive myoclonus epilepsies: Specific causes and diagnosis. *N. Engl. J. Med.* 315, 296–305.
42. Thompson, J. D., Higgins, D. G., and Gibson, T. J. (1994) ClustalW: Improving the sensitivity of progressive multiple sequence alignment through sequence weighting, position-specific gap penalties and weight matrix choice. *Nucleic Acids Res.* 22, 4673–4680.
43. Baker, N. A., Sept, D., Joseph, S., Holst, M. J., and McCammon, J. A. (2001) Electrostatics of nanosystems: Application to microtubules and the ribosome. *Proc. Natl. Acad. Sci. U.S.A.* 98, 10037–10041.
44. Pettersen, E. F., Goddard, T. D., Huang, C. C., Couch, G. S., Greenblatt, D. M., Meng, E. C., and Ferrin, T. E. (2004) UCSF Chimera-A visualization system for exploratory research and analysis. *J. Comput. Chem.* 25, 1605–1612.

BI801645Z